Additive Manufacturing 8 (2015) 78–87

Contents lists available at ScienceDirect

Additive Manufacturing

journal homepage: www.elsevier.com/locate/addma

An experimental demonstration of effective Curved Layer Fused Filament Fabrication utilising a parallel deposition robot

Robert J.A. Allen*, Richard S. Trask

Advanced Composites Centre for Innovation and Science (ACCIS), Department of Aerospace Engineering, University of Bristol, Queen's Building, University Walk, Bristol BS8 1TR, UK

ARTICLE INFO

Article history:
Received 2 February 2015
Received in revised form 1 July 2015
Accepted 16 September 2015
Available online 25 September 2015

Keywords:
Additive manufacturing
Rapid prototyping
Fused Deposition Modelling
Curved layer
Multi-material

ABSTRACT

Fused Filament Fabrication (FFF) is an additive manufacturing (AM) method that relies on the thermal extrusion of a thermoplastic feedstock from a mobile deposition head. Conventional FFF constructs components from stacks of individual extruded layers using tool paths with fixed *z*-values in each individual layer. Consequently, the manufactured components often contain inherent weaknesses in the *z*-axis due to the relatively weak thermal fusion bonding that occurs between individual layers, as well as poor surface finish in shallow sloped contours. This study demonstrates the use of Curved Layer FFF (CLFFF) tool paths in tandem with a commercially available parallel, or delta, style FFF system to allow the deposition head to follow the topology of the component. By incorporating a delta robot and CLFFF tool paths in this way, improvements in the surface finish of the manufactured parts has been observed, and time costs associated with Cartesian robot based CLFFF manufacturing have been notably reduced. Furthermore, employing a delta robot provides additional flexibility to CLFFF manufacturing and increases the feasibility of its application for advanced manufacturing. The study has also demonstrated a viable approach to multi-material FFF by decoupling support structure and part manufacture into regions of CLFFF and static *z* tool pathing in an appropriate fashion.

1. Introduction

Additive manufacturing (AM) offers a range of techniques for fabricating components with precise topologies from three dimensional CAD data. Current applications typically include high value manufacturing and prototyping, although as costs are reduced a broader assortment of applications is emerging and a number of AM consumer products are beginning to appear. In general AM processes rely on the consolidation of a feedstock material to produce physical components using a wide variety of methods that have been continually developed since they were initially envisaged several decades ago. These processes illustrate a distinct contrast when compared to traditional subtractive methods of advanced manufacturing and prototyping such as computer numerically controlled (CNC) machining where material is machined from a larger initial work piece in a precise fashion.

Nearly all AM processes rely on constructing components in a layered fashion, whereby 3D topological data is divided into a number of slices through the 'z' direction, and each layer of the component is consolidated sequentially from this data. The precise methods used in AM include a broad range of techniques, many of which are discussed in depth by Levy et al. [1] in their review of the state of the art methods currently in use. Although this expanding array of AM methodologies exists the majority can be divided into two distinct categories based on how new feedstock material arrives at the build plate in order to produce each sequential layer. The first method involves the use of a vat, or bath, of the feedstock material. In these processes a build plate is typically contained within the vat and a layer of feedstock material is evenly distributed across the full area of the build volume, typically in a liquid, or fluidised powder state. Each layer is then selectively solidified using a variety of techniques that include laser sintering or melting, deposition of a fluid binder, or exposure to UV radiation amongst others. These methods represent some of the most advanced and consistent techniques of AM currently available. Furthermore they also cover an impressive range of materials from engineering thermoplastics such as PolyEtherKetone (PEK) [2] to biocompatible titanium alloys that have been employed in medical applications, as studied by Vandenbroucke and Kruth [3].

The second group of AM methods tend to use a system whereby material is selectively deposited in precise geometries through a moving print head. Typically material is fed to the moving head

* Corresponding author.
E-mail address: R.J.A.Allen@Bristol.ac.uk (R.J.A. Allen).

http://dx.doi.org/10.1016/j.addma.2015.09.001

where it is deposited in extruded tracks that are bonded together in a variety of methods depending on the specific process in use. Print head deposition methods of AM cover a similarly wide range of available feedstock materials and resultant applications. For example Compton and Lewis [4] recently report the manufacture of small scale light weight cellular structures using a short fibre epoxy ink feedstock using a deposition based method of AM. In contrast, the study by Martina et al. [5] demonstrates the deposition of Ti–6Al–4V through plasma welding, with the aim of constructing large-scale aerospace components. One of the first, and perhaps the most common, print head based AM methods relies on the thermal extrusion and then fusing of a thermoplastic filament through a suitable extrusion nozzle. This method is often referred to as Fused Filament Fabrication (FFF), or Fused Deposition Modelling (FDM), and its low cost and simplicity has seen it emerge as the dominant AM method in the hobbyist market. Despite its low cost FFF boasts a range of available feedstock materials as well as more recently demonstrating the ability to manufacture multi-material components containing discreet regions of distinct materials. This approach provides print head deposition AM methods with a unique advantage over other AM techniques, where the process is often only limited to a single feedstock material. Multi material FFF components have begun to demonstrate added multi-functionality in manufactured parts that are desirable for a range of applications. An example is presented by Leigh et al. [6] where components are manufactured using a commercially available consumer dual material FFF system to deposit distinct regions of an electrically conducting and insulating thermoplastic. They demonstrated the manufacture of components containing embedded electrical circuits using this technique. Considerable advantages have also been identified when components containing materials of contrasting mechanical properties have been used to mimic biological structures observed in nature. Dimas et al. [7] demonstrate an example using polyjet technology where contrasting proprietary liquid monomer feedstocks are selectively deposited and polymerised in a precise structure. Mechanical testing of components manufactured using this technique, and consisting of bio-mimetic designs that imitate natural bone-like structures, have shown notable increases in fracture toughness. Other studies on the mechanical performance of FFF manufactured components have investigated the influence of tool pathing on material properties. Ahn et al. [8] conducted comprehensive testing of FFF test coupons constructed from acrylonitrile-butadiene-styrene (ABS). Their results indicate significant reductions in the tensile strength of FFF test coupons based on tool path orientation or raster. It can be concluded from these studies and others in the literature [9], that FFF components exhibit natural faults along thermal fusion boundaries between individual extruded tracks as well as layer interfaces. Conversely it has also been observed that the mechanical properties of FFF coupons approach that of equivalent injection moulded parts when applied loads are parallel to the raster orientation. This property of FFF components, and many other AM components, has led to inherent weaknesses in the z-axis of parts. These weaknesses can often manifest themselves as component failures due to the separation (delamination) of individually manufactured layers.

Curved Layer Fused Deposition Modelling (CLFDM), or CLFFF, describes a dynamic tool pathing method for FFF manufacturing. CLFFF tool paths contain dynamic z-values within individual layers in contrast to conventional FFF tool pathing where z-values remain static within each individual layer. This tool pathing technique was first discussed by Chakraboty et al. [10] who suggested algorithms for the generation of such tool paths. Although FFF is particularly suited to curved layer techniques another example of curved layer AM exists prior to investigations involving FFF. Klosterman et al. [11] developed a curved Layer Laminated Object Manufacturing (LOM) method and demonstrated the fabrication of curved components using a pre-manufactured mandrel and a modified commercial LOM system. The process relies on constructing complete individual layers from laser cut sheets and so is simpler than FFF approaches and consequently offers less flexibility to the user when compared to CLFFF. Even so, the study demonstrates significant advantages for specific applications when compared to traditional static z-layer LOM methodologies and demonstrates improvements in manufactured part quality and strength. Through the application of CLFFF tool pathing the mechanical performance of FFF components can also be enhanced in a dynamic surface, such as the skin of the component, as the tool path follows the surface geometry [12]. In addition to providing improved mechanical performance to the skin structure of FFF components, CLFFF can also help to improve surface smoothness. Step like structures that appear in the shallow sloping surfaces of parts manufactured using FFF as a result of individual layer boundaries have been studied and identified as a key factor in the surface finish quality of FFF parts [13]. By employing CLFFF it is possible to significantly reduce the effects of these step structures. Although CLFFF was first discussed in 2008, only limited experimental demonstrations of the technique exist in the literature, see for example the work by Huang et al. [14]. In this study, the authors demonstrate the manufacture of small test pieces using CLFFF; however, there experimental studies where limited as they employed a conventional Cartesian FFF system. Such Cartesian systems typically have z-axis speeds that are significantly lower than those that are capable in the x–y plane of the deposition head as the z-axis is required to move the full build platform. For example, a market leading consumer Cartesian FFF manufacturer recommends a maximum z-speed of $5\,\mathrm{mm\,s^{-1}}$ compared to $150\,\mathrm{mm\,s^{-1}}$ for the x and y axes [15]. Consequently manufacturing times when utilising CLFFF with traditional Cartesian systems is significantly increased when compared to conventional tool pathing techniques, as print head speeds are lower than the typical $50\,\mathrm{mm\,s^{-1}}$ when performing dynamic movements in the z-axis. Additionally the application of CLFFF using traditional Cartesian robots is further limited geometrically due to collisions that will occur between the print head, or gantry, and the component being manufactured during production of large components.

In this study CLFFF is demonstrated using a modified delta FFF system which removes the time penalty associated with Cartesian CLFFF techniques as the delta robot can attain print head speeds of up to $300\,\mathrm{mm\,s^{-1}}$ in all directions, whilst a speed of $50\,\mathrm{mm\,s^{-1}}$ is typically used during track extrusion movements [16]. Incorporating a delta robot also provides the FFF deposition head with increased movement capability consequently reducing the geometric constraints of CLFFF due to collisions, and increases the flexibility of the process. A further complication in FFF processing concerns manufacturing components with significant overhanging regions. Typically such regions are supported through the use of a support structure that is printed in tandem with each layer of the model and removed once manufacture is completed. Although effective supports have been manufactured using this method, this study also experimentally demonstrates an effective method of including support structures in FFF by combining traditional and CLFFF tool pathing which offers advantages in various geometric scenarios. Finally, FFF lends itself to multi-material AM through the use of print heads that contain multiple extrusion nozzles. Dual material FFF is highly desirable for a number of applications where additional functionality of components is advantageous. In our work, we experimentally demonstrate the benefits of using decoupled conventional and CLFFF tool paths to manufacture multi-material FFF parts containing discreet regions of contrasting materials. The process is conducted using only a single deposition head by performing feedstock changes between decoupled tool paths.

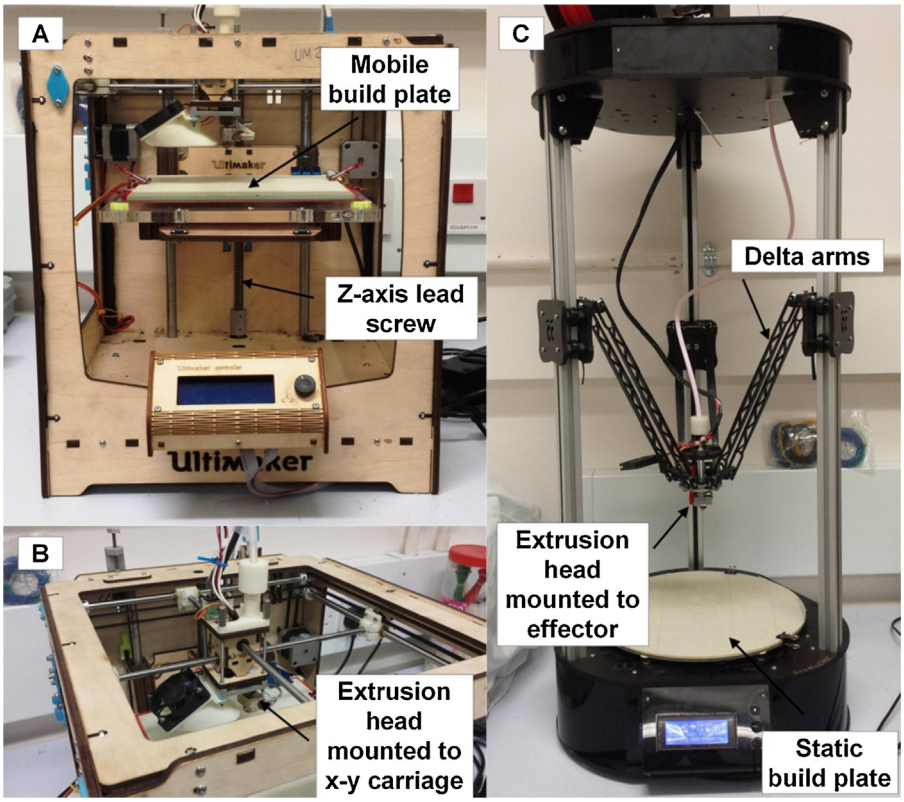

Fig. 1. A comparison of Cartesian and delta based FFF systems: (A) overview of a consumer Cartesian FFF system detailing the *z*-axis and mobile build plate; (B) detail of Cartesian *x*–*y* carriage; (C) overview of a delta style FFF detailing key components.

2. Materials and methods

2.1. Delta FFF system

In order to demonstrate CLFFF as a viable method of AM, the use of a delta style FFF robot was employed. Delta robots are often used in industry for pick and place tasks, and have recently been adapted for consumer FFF devices. Delta, or parallel, robot systems operate using three sets of parallel arm pairs to manoeuvre an effector plate to precise locations in 3D space. These systems have found increasing application since there initial development [17], but have only recently been applied in FFF. Delta robots offer a significant advantage over more traditional Cartesian FFF systems as all three axes offer identical speeds and precision. Cartesian systems often rely on a dual or single axis print head and typically utilise a mobile *z*-stage that lowers the build platform when moving to the next layer. In contrast, delta style robots can offer truly three dimensional movements of the print head within the build volume whilst the build platform remains stationary, consequently offering faster manufacturing speeds and increased accuracy. Fig. 1 illustrates the comparison between a consumer Cartesian based FFF system and a delta FFF system.

The delta FFF used in this studied is a Rostock MAX V2.0 (SeeMeCNC, Goshen, US, (http://seemecnc.com)) and is a standard consumer FFF system except for some minor modifications to convert the extruder to accept 3 mm feedstock filaments. These modifications involve the fitment of a typical 3 mm extruder nozzle and heater block, as well as the installation of a suitable Bowden tube fed 3 mm filament feeder system. The fitment of this extrusion nozzle also provides the system with sufficient clearance between the delta robots effector and the extrusion nozzle to demonstrate CLFFF capabilities. The original extruder system allows little clearance between the nozzle and effector plate in an effort to maximise the build volume of the system; however, this is unsuitable for use with CLFFF tool pathing. Fig. 2A displays the extruder nozzle as fitted to the Rostock FFF system, and Fig. 2B details the cut away schematic of the construction of the 3 mm extruder.

2.2. Curved Layer Fused Filament Fabrication tool pathing

An example of the application of CLFFF tool pathing can be demonstrated through the use of a simple sandwich panel example, consisting of both a skin and core component. Initially a simple curved surface is chosen that follows the surface plot of $f(z) = (\sin(x))^2 \times (\sin(y))^2$ for $[(0 \leq x \leq \pi), (0 \leq y \leq \pi)]$. This surface plot is then scaled to fill an area of 50 mm × 50 mm with amplitude of 9 mm. The skin structure is then extruded to have a thickness of 1.2 mm, equivalent to six individual extruded layers, and the core structure is considered to be the area bound below the skin in this case. Fig. 3 illustrates the CAD diagram of the structure of the simple part described above that is being used in this example, illustrating both skin and core components accordingly.

In typical FFF techniques CAD data is converted to a stack of individual layers of uniform thickness which are then deposited sequentially to produce a 3D component. Each individual layer is deposited from the print head by following a precise tool path with a static *z*-value that follows the part geometry in the *x*–*y* plane. A variety of software exists that can calculate conventional tool paths for FFF from CAD data and during this study the authors use the open source software Cura to generate appropriate conventional tool path files. Fig. 4A illustrates the tool path data generated by Cura (Ultimaker Inc., NL, http://Ultimaker.com) and visualised using RepetierHost (Hot-World GmbH & Co. KG, DL, (http://repetier.com)) software for the example component illustrated in Fig. 3. The tool path is generated to have a typical *z*-layer thickness of 200 μm and an extrusion track width of 400 μm

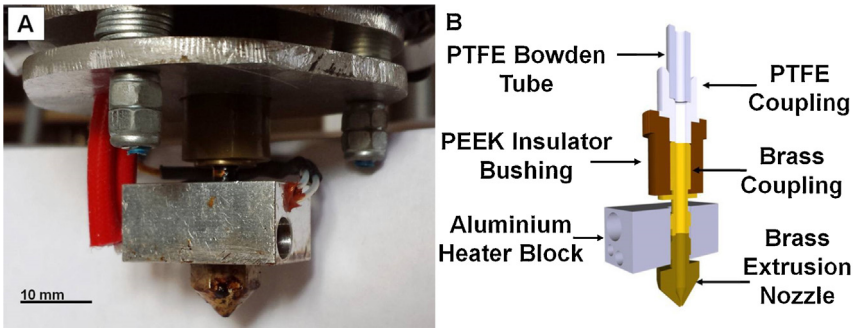

Fig. 2. FFF extrusion nozzle mounted to the effector plate of the delta system used in this study: (A) extrusion nozzle mounted in situ; (B) cut away schematic detailing key components of the extruder system.

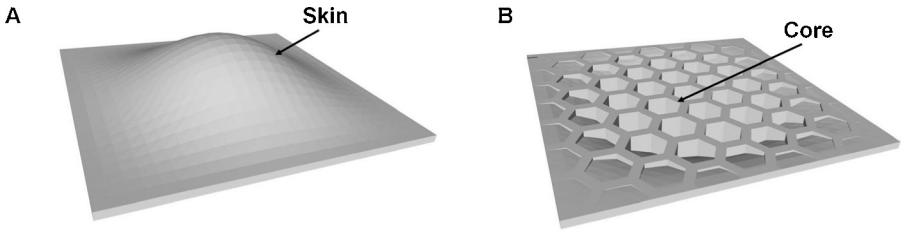

Fig. 3. CAD render images of a simple part used to demonstrate CLFFF tool pathing: (A) view illustrating the skin surface; (B) inverted view of (A) detailing the underlying core structure of the component.

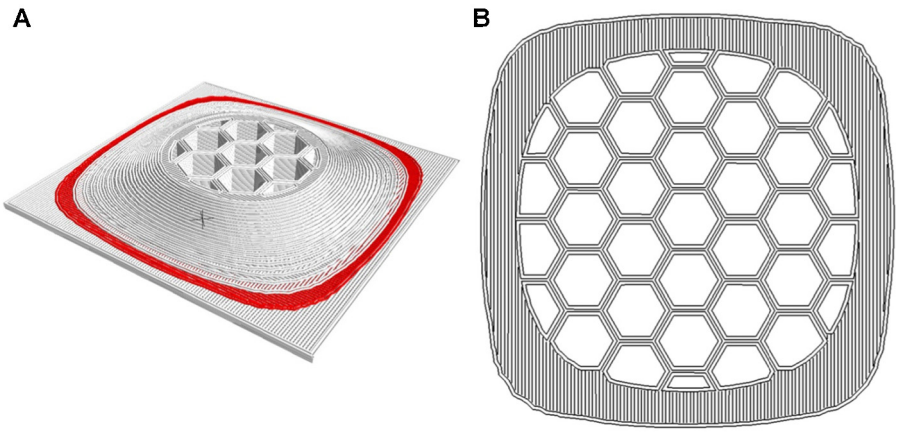

Fig. 4. Conventional FFF tool path generated using Cura for the simple part illustrated in Fig. 3: (A) Complete tool path visualisation with upper section removed to detail internal structure; (B) Visualisation of an individual layer tool path, this layer is highlighted in red in (A). (For interpretation of the references to color in figure legend, the reader is referred to the web version of the article.)

which is typical for consumer FFF processes. Fig. 4B provides the clearer visualisation of the tool path for a single layer demonstrating how the component is manufactured from individual extruded tracks, and both skin and core structures are manufactured simultaneously.

In order to incorporate CLFFF tool pathing it is necessary to split the CAD model into distinct parts that can be printed using conventional tool pathing and CLFFF tool pathing respectively. In this case the part is split into a core structure and a skin plane as detailed previously in Fig. 3. To simplify the process the core structure tool path is generated in an identical fashion to the previous example using the Cura software package. This part of the component is the first to be manufactured and provides the support for the CLFFF skin component to be printed over. Fig. 5A illustrates the visualisation of the conventionally generated core tool path. As discussed earlier, methods to calculate CLFFF tool paths have been investigated previously [10,14], and are similar to tool paths that are currently generated in various advanced CNC manufacturing techniques. Despite this, current CLFFF tool path generators have seen only limited experimental validation in the literature [12] that can likely be attributed to the impracticality of the technique when using Cartesian FFF systems. Consequently in order to allow accurate refinement of the critical FFF manufacturing parameters this study uses a simple mathematical approach to CLFFF tool path generation designed specifically for this experimental study. To generate tool paths the surface is converted to an array of data points in the x–y plane over a grid of equal size to the surface and resolution equal to the extrusion track width; in this simple case, a 50 mm × 50 mm square with 400 μm resolution. z-Values can then be calculated for each point using the surface equation and creating a vector field that follows the data points sequentially. This vector field is then converted to an appropriate tool path file that contains dynamic z movements and extrusion values calculated from individual vector magnitudes. Using this simple generator raster orientations are limited to 0° and 90° within the plane of the surface although potential exists for the manufacture of skin layers that could contain many raster

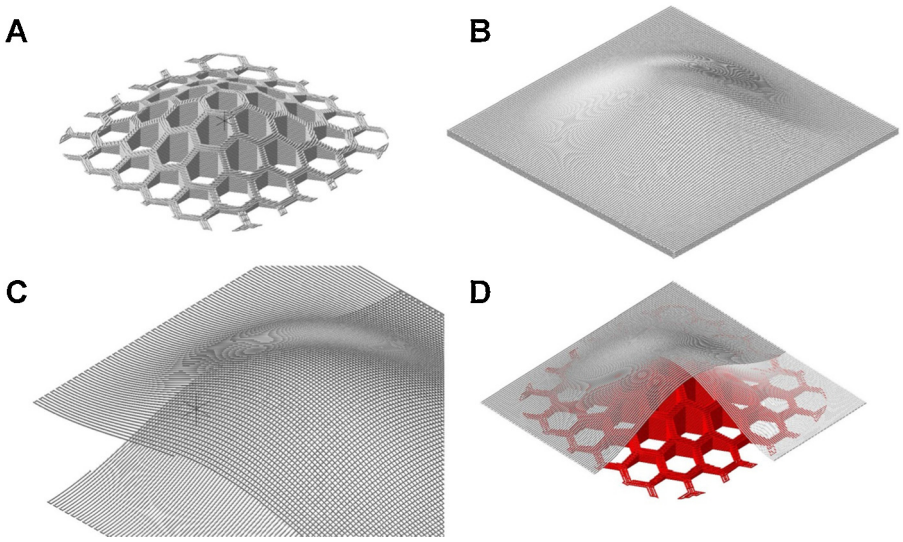

Fig. 5. Tool path visualisation for the simple part example using both conventional and CLFFF components: (A) visualisation of conventional tool path of path for the core structure; (B) complete CLFFF tool path visualisation of the skin structure; (C) section of CLFFF tool path illustrating the individual layer raster orientations; (D) combined visualisation illustrating how CLFFF tool paths are supported by the conventional core structure.

orientations using more complex tool pathing techniques. Fig. 5B and C shows the visualisations of the CLFFF tool path demonstrating the full tool path, and a small section illustrating the raster orientation respectively, and finally Fig. 5D details the combined tool paths used to manufacture the component. In this example CLFFF layers are generated to be 200 μm in thickness and 400 μm in width and the skin layer consists of 6 individual CLFFF layers.

The visualisations in Figs. 4 and 5 clearly demonstrate the benefits of CLFFF tool pathing when compared to conventional tool pathing methods, but also highlights some limitations of the technique. By using CLFFF tool paths step like structures, that are often visible in shallow sloped surfaces of components fabricated using FFF, can be significantly reduced. By removing these typical layer steps using CLFFF the manufacture of smoother sloped surfaces is viable, and improved mechanical performance of such surfaces is predicted and has been demonstrated in the literature previously to some extent [12,14]. The generation of CLFFF tool paths as detailed contains inherent restraints due to the requirement of avoiding collisions between the print head and part being manufactured. Consequently some minor modifications of tool paths are necessary to ensure sufficient clearance of the print head during the manufacturing process; however, such movements are relatively simple when using a delta FFF system compared to a typical Cartesian robot. A similar modification to avoid collisions has been conducted by another group [18] previously to good effect when conducting conventional FFF on freeform surfaces, although this study used a Cartesian robot and static *z* tool pathing techniques.

3. Case studies

3.1. Simple skin surface and core example

Our first case study example demonstrates FFF manufacturing of the CAD file detailed in Fig. 3 produced using CLFFF tool pathing as visualised in Fig. 5. This relatively simple geometry can also be manufactured using a conventional tool path as detailed in Fig. 4 and thus a comparison between both methods can be drawn. Both parts are manufactured using a Rostock MAX delta FFF system, as detailed in Fig. 1, and are produced using a polylactide (PLA) thermoplastic feedstock material, NatureWorks – 2002D. Fig. 6A and B illustrates the comparison of images of both the manufactured parts. The images demonstrate a visible improvement in the surface finish of the component produced using CLFFF when compared to the conventional part. The improved surface of the CLFFF part is apparent in regions where the gradient of the slope is shallow thus magnifying the step effect.

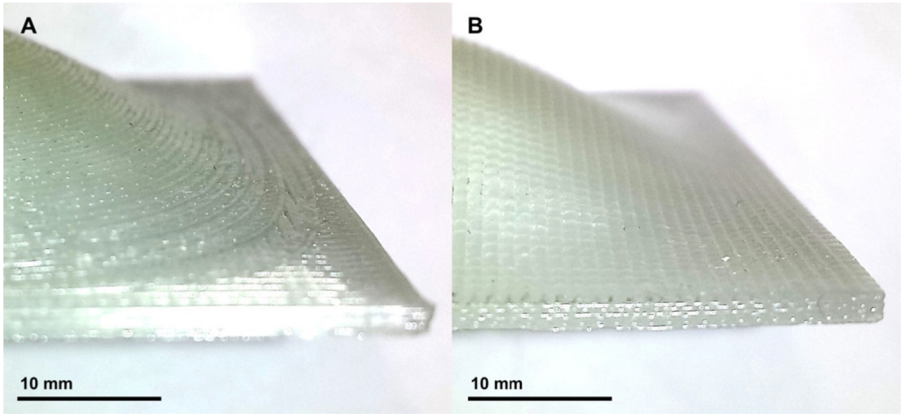

Fig. 6. Images of sloped regions of the simple example parts manufactured using contrasting tool path techniques for FFF as part of this study: (A) component manufactured using conventional tool pathing; (B) component with skin layer manufactured using CLFFF tool pathing, demonstrating improved skin structure.

Table 1
Measured and calculated total manufacturing times for the first case study using different tool pathing strategies.

Geometry	Tool pathing strategy	Source	Manufacturing time (s)	Percentage of skin + core conventional manufacturing time (%)
Skin + core	Conventional (skin + core)	Experiment	1960	100
Core	Conventional	Experiment	818	41.7
Skin + core	Conventional (core) + CLFFF (skin)	Experiment	1630	83.2
Skin	Conventional	Calculated (row 1 – row 2)	1142	58.3
Skin	CLFFF	Calculated (row 3 – row 2)	812	41.4

Using this simple CAD design also allows a direct comparison between manufacturing speeds for both tool pathing methods. Table 1 lists total print times for skin, core and combined geometries manufactured using different tool pathing strategies. By using a delta FFF system it is possible to use the maximum recommended volumetric feedstock extrusion rate for the deposition head which corresponds to a print head speed of 50 mm s^{-1} at 200 μm layers for both tool pathing techniques. The results indicate that manufacturing speeds using CLFFF are comparable to conventional tool pathing, and in this simple example CLFFF tool pathing has reduced total manufacturing time by ~17%, as CLFFF tool paths generated in this study contain no travel moves. Despite the reduction in manufacturing times observed in this case, it is expected that CLFFF manufacturing times will be similar to those of conventional FFF when manufacturing more detailed arbitrary surfaces, as travel moves will be integral to the more complex tool path generator required in this case. Even so, the results in Table 1 demonstrate successful CLFFF at speeds far greater than those possible using Cartesian based FFF systems owing to the limited print speeds of these systems discussed previously.

Previous works have also attempted to improve surface quality of FFF components using a variety of methods, for example Lee et al. [19] incorporate a CNC mill into a Cartesian FFF system allowing parts to be milled after manufacture improving the finish of part surfaces. A further example exists in another study [20] where a hot blade edge was utilised to smooth the outer surface in a similar fashion although this process is limited to flat surface geometries owing to the blades profile. Both methods demonstrate improvements in surface finish however both significantly increase manufacture time through incorporating an additional post processing stage to the AM process. In contrast using CLFFF tool pathing in tandem with a delta FFF system can achieve similar improvements with little increase in manufacturing time as demonstrated and detailed in Table 1. Employing CLFFF tool pathing can also provide improvements in mechanical performance by taking advantage of the anisotropic properties of FFF components which cannot be achieved using post processing methods. It should be recognised that some step effects are still present in the CLFFF component, imaged in Fig. 6B, that occur as a result of the inherent steps in the CLFFF tool path raster. These steps cause a smaller effect in part surface topology as they have a fixed resolution of 400 μm, which is equal to the deposition nozzle diameter, in contrast to conventional tool paths where the step resolution is directly related to the incline of the surface in question.

3.2. A sinusoidal multi-material sandwich panel structure

Thus far only a basic use of CLFFF tool pathing has been demonstrated, however the authors note that with careful planning further advantages can be gained by employing CLFFF tool pathing to more complex components. In this example a sinusoidal sandwich panel structure is devised, where a conventional honeycomb core of 10 mm thickness is enclosed between two 2 mm thick sinusoidal skin layers to be constructed using CLFFF tool pathing. The skin layers follow the form of $f(z) = \sin(x) \times \sin(y)$ for $[(3\pi/2 \leq x \leq 11\pi/2), (\pi/2 \leq y \leq 9\pi/2)]$ with sinusoidal peaks in the surface having an amplitude of 9 mm from peak to trough. The overall size of the panel is 100 mm × 100 mm × 23 mm although the in-plane thickness of the panel is only 14 mm at any given point. A CAD representation of the desired part geometry is demonstrated in Fig. 7, clearly displaying the incorporation of the dynamic surfaces on the upper and lower skin surfaces of the structure.

In order to manufacture this more complex structure the incorporation of a support structure is required to ensure accurate manufacturing of the lower skin layer. By manufacturing different sections of the part using conventional and CLFFF tool pathing respectively an effective method of incorporating support materials is demonstrated. The process consists of two individual manufacturing processes that are conducted sequentially. The first process is to print a supporting raft structure that serves to support the lower skin CLFFF layers. This support structure provides a similar role to that of the mandrel supports used in the curved LOM process employed by Klosterman [11]. In conventional single material FFF support structures are used to support overhanging regions of the part that would otherwise prove difficult to manufacture. These supports are typically printed as part of the overall structure and appear in each individual layer as required. In single material systems they are often manufactured from the same material as the part and can be difficult to remove leading to a detrimental effect on the part's surface quality. FFF incorporating more effective support structures has been demonstrated using dual material FFF

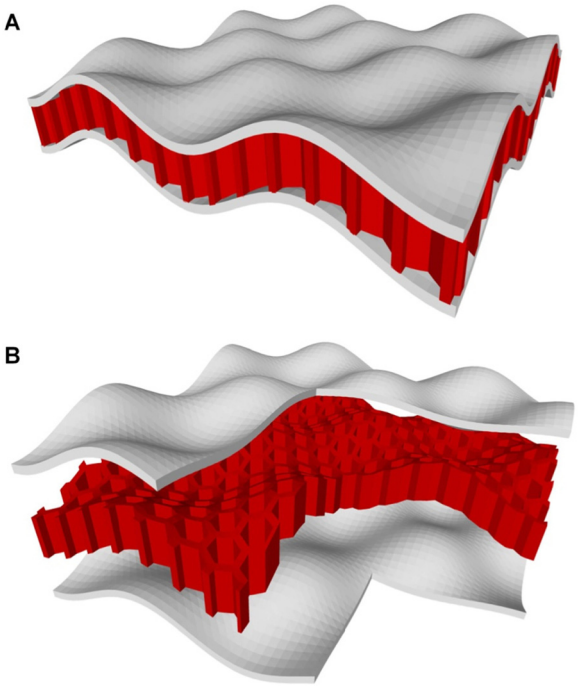

Fig. 7. CAD renders of the curved sandwich panel structure being used to demonstrate CLFFF tool pathing capabilities: (A) complete assembled sandwich panel structure; (B) exploded and cut away image of the curved sandwich panel revealing the honeycomb core structure.

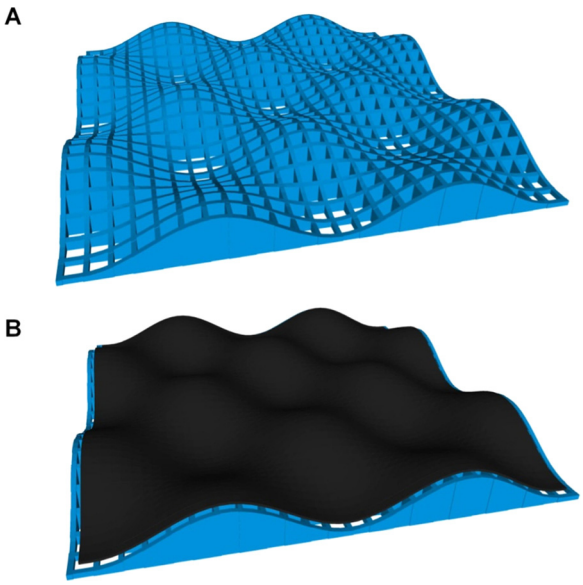

Fig. 8. CAD renders of support structures used in the manufacture of the curved sandwich panel structure: (A) render of the raft structure; (B) combined render of the raft structure and buffer layer.

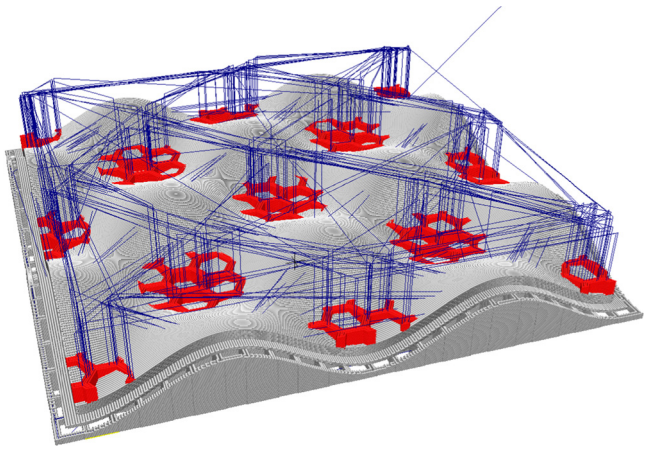

Fig. 9. Tool path visualisation of the core structure manufacturing stage. White paths represent the previously manufactured support structures and the lower skin layer and red paths represent the conventional tool path of the core structure. The dark blue paths represent travel moves where no extrusion occurs. It should be noted how vertical moves are performed prior to horizontal moves in order to avoid collisions; such sufficiently fast movements are only viable using a delta FFF system. (For interpretation of the references to color in figure legend, the reader is referred to the web version of the article.)

systems where a second nozzle is used to extrude a suitable support material that is easier to remove when manufacturing is completed. Typically, suitable support materials consist of a soluble polymer feedstock that can be dissolved after the manufacturing process is completed. Despite effective results being observed through the use of soluble supports the method relies critically on the use of dual extrusion systems. In this study we demonstrate a method using CLFFF tool pathing to print directly over a support structure that is manufactured fully before part production commences. Printing the support structure in this way allows the support to be printed faster and at a lower quality than the rest of the structure, and can also allow the support structure to be printed from a different material when using a single material FFF system. In this example a second step is incorporated into the raft structure that involves the use of a buffer layer that is printed in between the raft and the part itself. This layer is printed utilising a CLFFF tool path following an identical surface topology to the lower skin of the part but extending 2 mm out from the edges of the part in order to fully support the layer during deposition. The CAD visualisation of the raft structure is depicted independently in Fig. 8A, and with the added buffer layer in Fig. 8B.

By manufacturing FFF components that comprise of decoupled sections of unique tool pathing with both conventional and CLFFF components a method of multi-material FFF using a single deposition head exists. This can be achieved by performing manual material changes whilst pausing the manufacturing process. In this study the process is demonstrated through a simple manual material change and consequent purge of the extrusion nozzle. Manufacture is then resumed by printing a priming skirt before returning to the relevant section of the tool path file. Multi-material FFF through feedstock material changes has been demonstrated previously [18]; however, it is only through the use of CLFFF tool pathing that regions of each material can extend through the z thickness of the component. In this example the raft structure is printed using a coloured PLA as it offers fast accurate FFF manufacture at a low cost. The buffer layer is then manufactured using a proprietary ThermoPlastic Elastomer (TPE) feedstock (Fenner Drives Inc., US, (http://fennerdrives.com)) that is Polyurethane (PU) based. This layer functions as a release coating between the component and the supporting raft structure. The PU based TPE performs well as a release layer owing to the poor thermal fusion bonding that occurs between PLA and PU thermoplastic feedstocks during FFF. It is used in this case to demonstrate the benefits of multi-material capability due to its availability, although it could be substituted with a number of other suitable materials, such as a suitable soluble feedstock, which could be dissolved to release the manufactured component. A further advantage of manufacturing a PU buffer layer using CLFFF is that it provides an exact replica surface for the manufacture of the lower skin surface, reducing detrimental effects on surface quality that often result from the use of conventionally printed support structures that contained stepped edges. Once the buffer layer is completed the manufacture of the part begins and the lower skin is extruded directly over the support structure. In this case study the lower skin is manufactured by performing a material change to a natural PLA feedstock before initiating the progress; however, potential exists to use any available FFF feedstock material. The next stage of the manufacturing process is to produce the core structure of the component that will be manufactured directly onto the lower skin layer. The structure of the core is a simple Boolean subtraction of the void formed between the skin layers and the chosen core structure, in this case a simple hexagonal lattice. In order to effectively manufacture the core structure the FFF extruder head must accurately travel between individual islands of the core structure whilst avoiding collisions. This stage can only be effectively achieved using a delta FFF process, as high speed motion of the 'z-axis' is required to perform effective movement of the extruder between different regions without significant 'seepage' of feedstock material. This process is demonstrated experimentally for the first time in this study and is observed to be effective in manufacturing components of comparable quality to conventional FFF techniques. Fig. 9 illustrates an example tool path visualisation demonstrating how this hopping motion is incorporated to a conventional tool path in order to manufacture the core structure.

In this example, the core structure is constructed with a similar PLA to that used previously but containing a red colourant to clarify the different regions of the manufacturing process. In order to manufacture the core in this style a manual feedstock change is conducted, although this process would not be required if the core and skin structures were to be constructed from the same feedstock material as in the first example in this study. Finally when the core is completed the top skin layer can be manufactured. In this

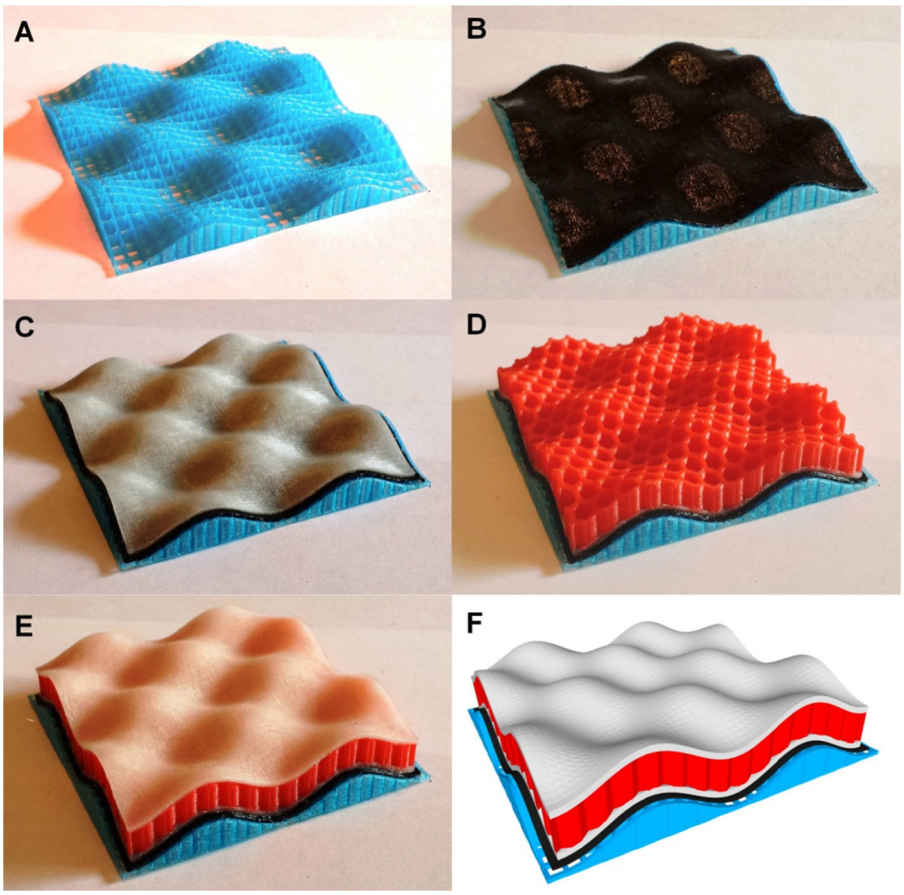

Fig. 10. Images and comparative render of curved sandwich panel manufacture: (A) raft structure; (B) buffer layer; (C) lower skin layer; (D) hexagonal honeycomb core structure; (E) upper skin layer; (F) comparative CAD render.

example, for simplicity, the upper skin layer is chosen to be identical to the bottom skin layer although it could follow a different surface topology to that of the lower skin if desired. The hexagonal core structure provides a suitable raft to allow manufacture of the upper skin directly on to the core surface although some small defects are present in the initial layers owing to the bridging of the individual hexagonal cells, as observed by others previously [21]. The effect of these defects can be reduced by decreasing the individual cell size of the core structure although this will in turn increase the density of the overall components structure, and therefore total print times. Fig. 10A–F details the schematic of the manufacturing process conducted in this study, illustrating images of each of the five individual stages of the component during manufacture.

When the manufacturing process has completed the raft material and buffer layer can be easily removed in a mechanical fashion to reveal the finished component. The raft structure is designed to be broken into small sections to aid simple mechanical removal from the component and buffer layer. With the raft structure removed it is then possible to mechanically peel the buffer layer from the lower skin owing to the poor thermal fusion bonding between the PU and PLA feedstocks. Fig. 11A illustrates the removal of the PU buffer layer; it can be peeled from the component without fracturing owing to its elastomeric properties. As this part has been designed to demonstrate the advantages of CLFFF tool pathing it is not possible to provide an effective comparison between a similar component manufactured using conventional tool pathing as shown in Fig. 6 previously. Despite this the quality of the component as manufactured and with support material removed can be seen in Fig. 11B and is of similar aesthetic quality to that observed in the first example included in this study. Some small defects can be seen in the lower surface in Fig. 11 when compared to the upper surface in Fig. 10. These defects probably result from the use of the buffer layer and could be improved by using a thicker buffer layer that is manufactured from a soluble feedstock material rather than one that is mechanically removed.

4. Discussions

4.1. Limitations of CLFFF tool pathing with a delta FFF system

This study utilises two distinct example geometries to demonstrate the potential of incorporating CLFFF tool pathing to FFF manufacturing through the use of a delta FFF system. Both structures contain sinusoidal surfaces that have been selected as they incorporate a range of gradients across the components surfaces. Consequently, the manufacturing of these geometries has demonstrated the effectiveness of CLFFF tool pathing across varying topologies. Although these examples demonstrate useful CLFFF capabilities it is clear that there are inherent limitations to the surfaces to which the process can be applied. In this study a typical thermoplastic filament extruder has been used, as detailed in Fig. 2, in order to avoid significant modification from a conventional FFF system. Using this extruder limits the maximum slope of incline to approximately 40° owing to the shape of the brass extrusion nozzle. As well as constraints due to nozzle geometry, a further problem exists relating to the distortion of the cross section of extruded tracks as result of interference with the deposition nozzle. This occurs as the extruder axis is no longer normal to the deposition surface with nozzle interference being more severe

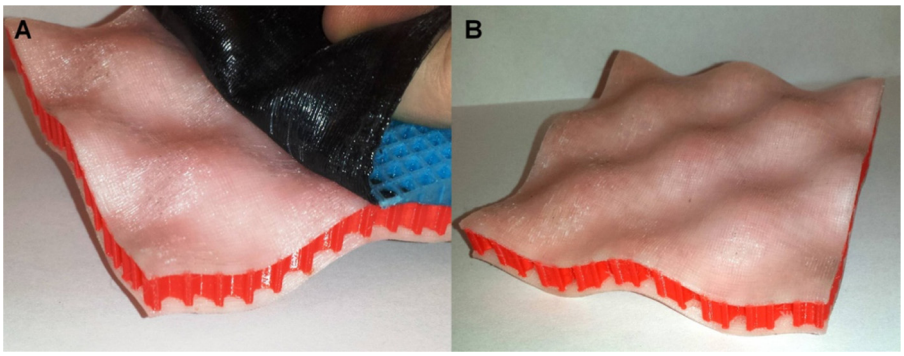

Fig. 11. Removal of the raft structure and buffer layer from the manufactured curved sandwich panel: (A) mechanical removal of the buffer layer from the lower surface of the panel; (B) overview of the lower surface of the part.

at steeper inclines. In this study the track width is 400 μm and thickness is 200 μm, and results demonstrate effective deposition on slopes of inclines up to 30°. Even so it should be noted that increasing the ratio of track width to layer thickness may reduce the maximum slope of incline possible without significant distortion of the track cross section. A solution to track distortion is to maintain normality between the extruder axis and dynamic surface during CLFFF manufacturing. Although not feasible with the current system in use, robots with sufficient degrees of freedom have demonstrated this technique in recent studies. For example the use of a simple 6-axis Stewart platform robot for CLFFF [22], and the embedding of wires on curved surfaces using a mobile rotating stage in tandem with a mobile print head [23]. Both studies have demonstrated low cost approaches to this problem, although they require additional mechanical and computational complexity than the method used in this study. Furthermore, the nozzle is not the only limiting factor to the maximum slope of incline. Even though the use of a delta robot removes the possibility of collisions with the print head gantry, as possible in Cartesian systems, it is important to consider that when manufacturing large components the entire deposition head, including the effector plate can collide with the part. Evidently modifying the extrusion nozzle and deposition head structure to consist of a narrower geometry will allow better accessibility of the print head to the part surface and theoretically can increase the maximum possible incline of the surface although in depth investigations into the maximum possible slope of incline are still required. Even with the implementation of these various modifications to improve the range of suitable surfaces for the application of CLFFF it remains that the best improvements in quality will be observed in relatively shallow sloping curved surfaces. Furthermore it is also apparent that certain geometries will never be suitable for the application of CLFFF tool pathing using a delta robot although many designs will contain regions that are suitable for manufacturing using this method.

As well as physical limitations relating to the structure of the extruder only a simple algorithm has currently been used to generate the CLFFF tool paths for the skin structure. This process relies on computing dynamic z-values numerically as the surfaces used are of a mathematical form allowing calculation of the appropriate z-values. In order for viable tool paths to be generated the surface is divided into a rectangular grid of point data with a spacing that is equal to the extrusion track width. Each point can then be defined in three dimensions and tool paths create by following the point data field. Consequently, the current tool path generation technique can only be applied to rectangular surfaces that follow a mathematical form. Furthermore the raster orientation of these surfaces is currently limited to 0/90° directions which are adequate for the manufacture of smooth surfaces in this case, however it may be of benefit to incorporate user defined raster orientations to the tool path generation process. These methods provide an example for refining the CLFFF process using a delta system, but it is clearly desirable to be able to incorporate CLFFF tool pathing to the FFF of arbitrary free form surfaces in order to suit variety of applications. As discussed, some literature exists that demonstrates freeform CLFFF tool path generation software and some commercial products are currently under development [24], but no suitable CLFFF tool path generation software was available at the time of this study. Using the results from this study an algorithm to incorporate these features is currently being developed at Bristol and is undergoing early experimental testing. This algorithm was not used in this work as numerical generation of tool paths currently allows a more precise generation of tool paths that is desired in this initial experimental phase.

4.2. Applications of CLFFF tool pathing

Neither example used in this study has any specific application but rather exhibits a useful demonstration of manufacturing capability with CLFFF tool pathing. Example components were chosen to be compatible with the current tool path generation method, but still demonstrate a range of surface topologies. As discussed, the applications of CLFFF tool paths maybe limited owing to design limitations in topology of part surfaces however the authors have identified some key areas that could benefit from this unique tool pathing technique. These applications focus on maximising the benefits of employing CLFFF whereby improvements in skin surface quality and strength are vital to the function of the component. Such examples include a variety of applications in the aerospace and automotive industries where many sandwich panel structures are currently being employed to provide superior mechanical function at a low weight cost. It is also frequently desirable for these panels to follow precise topologies that can be manufactured simply using the FFF process. The fabrication of such components in a decoupled fashion through the use of CLFFF tool pathing offers a further advantage. In this study, a uniform hexagonal honeycomb core structure has been chosen to best represent typical sandwich panel compositions. However, the core structure has the potential to be manufactured to any desired geometry that is suitable for conventional FFF manufacturing. For example it may be desirable to include a functional grading of the core geometry in order to introduce varying stiffness to the components overall structure. These capabilities are of particular advantage in scenarios where weight is at a premium but mechanical performance is also desired such as in modern unmanned aerial vehicle (UAV) components. Another application may be found in personal armour where it may be desirable to print skin layers that follow the contour of an individual's form and size to provide an improved user fit.

An application of particular interest to the authors is the incorporation of composite feedstocks to the FFF process that offer increased mechanical performance of components in the raster

orientation. A number of short fibre reinforced thermoplastic feedstocks have previously been developed for use in unmodified FFF systems. Zhong et al. [25] demonstrate that the addition of up to 20 wt% of short glass fibres can improve the tensile strength of FFF components in the extrusion direction by up to 100%. Combining short fibre composite material feedstocks with CLFFF tool paths offers the potential to align short fibre reinforcements within the surface of the skin layer. In doing so it is predicted from the results of other studies [9,11,12,14], that an increase in the mechanical performance of the skin surface can be achieved that will further increase the improvement over conventional FFF skin structures. Preliminary investigations into CLFFF manufacturing using composite feedstocks have been discussed previously and have demonstrated some potential for the controlled alignment of fibre composites in CLFFF components [26,27], although further studies are required to fully investigate this field. As well as composite materials for FFF applications CLFFF tool paths could also be applied to a range of similar print head based additive manufacturing techniques. Consequently the potential to apply these techniques to systems that use a wide range of feedstock materials exists. However, further investigation and likely significant modification to current processes will be required to investigate the suitability of this method to such techniques. Even so, current additive manufacturing research is leading towards increased flexibility that may facilitate the incorporation of CLFFF tool path methods in the future.

5. Conclusions

This study demonstrates the generation of a variety of tool paths that contain CLFFF components for use in manufacturing with a delta style FFF system. CLFFF tool pathing allows the manufacture of free form surfaces where individual tool paths map the surface topology. Experimental results have demonstrated effective manufacturing through the use of decoupled skin and core tool paths made possible through the flexibility of the delta FFF system. Manufactured parts demonstrate improved surface finish compared to conventional FFF parts that are known to contain step structures in shallow sloping regions. As well as improvements in surface finish, mechanical property enhancements of the skin surface are also expected. Furthermore, through combining CLFFF and a delta system increased print times previously associated with Cartesian CLFFF that result from low *z*-axis movement speeds have been minimised. In addition CLFFF also demonstrates an alternative method of producing support structures for FFF and improvements in supported surface quality have been observed. Finally an approach to the inclusion of multiple materials during FFF has been demonstrated which has the potential to offer additional functionality to parts. For example, in this study the skin and core components of the sandwich panel could be constructed from contrasting materials that offer distinct structural or physical functions to each component respectively.

Acknowledgements

The authors gratefully acknowledge the support of the EPSRC for funding RST's fellowship and research under EPSRC 'Engineering Fellowships for Growth', Grant number EP/M002489/1.

References

[1] G.N. Levy, R. Schindel, J.P. Kruth, Rapid manufacturing and rapid tooling with layer manufacturing (LM) technologies, state of the art and future perspectives, CIRP Ann.: Manuf. Technol. 52 (2003) 589–609.
[2] O. Ghita, E. James, R. Davies, S. Berretta, B. Singh, S. Flint, K.E. Evans, High Temperature Laser Sintering (HT-LS): an investigation into mechanical properties and shrinkage characteristics of Poly (Ether Ketone) (PEK) structures, Mater. Des. 61 (2014) 124–132.
[3] B. Vandenbroucke, J.P. Kruth, Selective laser melting of biocompatible metals for rapid manufacturing of medical parts, Rapid Prototyp. J. 13 (2007) 196–203.
[4] B.G. Compton, J.A. Lewis, 3D-printing of lightweight cellular composites, Adv. Mater. 26 (2014) 5930–5935.
[5] F. Martina, J. Mehnen, S.W. Williams, P. Colegrove, F. Wang, Investigation of the benefits of plasma deposition for the additive layer manufacture of Ti–6Al–4V, J. Mater. Process. Technol. 212 (2012) 1377–1386.
[6] S.J. Leigh, R.J. Bradley, C.P. Purssell, D.R. Billson, D.A. Hutchins, A simple, low-cost conductive composite material for 3D printing of electronic sensors, PLoS ONE 7 (2012) e49365.
[7] L.S. Dimas, G.H. Bratzel, I. Eylon, M.J. Buehler, Tough composites inspired by mineralized natural materials: computation, 3D printing, and testing, Adv. Funct. Mater. 23 (2013) 4629–4638.
[8] S.H. Ahn, M. Montero, D. Odell, S. Roundy, P.K. Wright, Anisotropic material properties of fused deposition modeling ABS, Rapid Prototyp. J. 8 (2002) 248–257.
[9] C. Bellehumeur, L. Li, Q. Sun, P. Gu, Modeling of bond formation between polymer filaments in the fused deposition modeling process, J. Mater. Process. Technol. 6 (2004) 170–178.
[10] D. Chakraborty, B.A. Reddy, A.R. Choudhury, Extruder path generation for curved layer fused deposition modeling, Comput. Aided Des. 40 (2008) 235–243.
[11] D.A. Klosterman, R.P. Chartoff, N.R. Osborne, G.A. Graves, A. Lightman, G. Han, A. Bezeredi, S. Rodrigue, Development of a curved layer LOM process for monolithic ceramics and ceramic matrix composites, Rapid Prototyp. J. 5 (1999) 61–71.
[12] S. Singamneni, A.R. Choudhury, O. Diegel, B. Huang, Modeling and evaluation of curved layer fused deposition, J. Mater. Process. Technol. 212 (2012) 27–35 (Rapid Prototyp. J. (1999) 5(2), 61–71).
[13] B. Vasudevarao, D.P. Natarajan, M. Henderson, A. Razdan, Sensitivity of RP surface finish to process parameter variation, Sol. Freeform Fabric Proc. (2000) 251–258.
[14] B. Huang, S. Singamneni, Alternate slicing and deposition strategies for fused deposition modeling of light curved parts, J. Achiev. Mater. Manuf. 55 (2012) 511–517.
[15] https://ultimaker.com/en/products/ultimaker-original (accessed January 2015).
[16] http://seemecnc.com/products/rostock-max-complete-kit (accessed June 2015).
[17] R. Clavel, A fast robot with parallel geometry, in: Proc. Int. Symposium on Industrial Robots, 1998, pp. 91–100.
[18] J.W. Choi, F. Medina, C. Kim, D. Espalin, D. Rodriguez, B. Stucker, R. Wicker, Development of a mobile fused deposition modeling system with enhanced manufacturing flexibility, J. Mater. Process. Technol. 211 (2011) 424–432.
[19] W.C. Lee, C.C. Wei, S.C. Chung, Development of a hybrid rapid prototyping system using low-cost fused deposition modeling and five-axis machining, J. Mater. Process. Technol. 214 (2014) 2366–2374.
[20] P.M. Pandey, N.V. Reddy, S.G. Dhande, Improvement of surface finish by staircase machining in fused deposition modelling, J. Mater. Process. Technol. 132 (2003) 323–331.
[21] B. Huang, S. Singamneni, A mixed-layer approach combining both flat and curved layer slicing for fused deposition modelling, Proc. IMechE Part B: J. Eng. Manuf. (2014), http://dx.doi.org/10.1177/0954405414551076.
[22] X. Song, Y. Pan, Y. Chen, Development of a low-cost parallel kinematic machine for multidirectional additive manufacturing, J. Manuf. Sci. Eng. 137 (2015) 021005.
[23] C. Kim, D. Espalin, A. Cuaron, M.A. Perez, M. Lee, E. MacDonald, R.B. Wicker, Cooperative tool path planning for wire embedding on additively manufactured curved surfaces using robot kinematics, J. Mech. Robot. 7 (2015) 021003.
[24] http://www.topolabs.com/ (accessed January 2015).
[25] W. Zhong, F. Li, Z. Zhang, L. Song, Z. Li, Short fiber reinforced composites for fused deposition modeling, Mater. Sci. Eng. 301 (2001) 125–130.
[26] S. Singamneni, O. Diegel, B. Huang, I. Gibson, R. Chowdhury, Curved-layer fused deposition modelling, J. New Gener. Sci. 8 (2010) 95–107.
[27] I. Gibson, Y. Liu, M.M. Savalani, L.K. Anand, Composites in rapid prototyping, J. New Gener. Sci. 7 (2009) 35–47.